Proceedings of the ASME 2016 Power and Energy
POWERENERGY2016
JUNE 26-30, 2016, Charlotte, North Carolina

POWERENERGY2016-59341

OPTIMAL CAPACITY SIZING FOR A COMPLETELY GREEN VILLAGE WITH PROGRAMMABLE APPLIANCES

Juliette Ugirumurera
Department of Computer Science
University of Texas at Dallas
Richardson, Texas, USA

Zygmunt J. Haas
Department of Computer Science
University of Texas at Dallas
Richardson, Texas, USA

ABSTRACT
Current trends show that renewable energy production costs continue to decrease with time, so that renewable energy sources (RES) are becoming more suitable as electricity sources. In addition to their environmental benefits, RES are especially appropriate for remote areas, where the expansion of existing power grid is impractical and fuel transportation for thermal generators is too expensive. In this regard, our work studies the optimal capacity sizing for a completely green village (CGV), which is an isolated residential microgrid (MG) whose power is entirely generated by RES. In particular, we consider a neighborhood composed of smart homes that contain programmable appliances, whose operations can be interrupted or automatically scheduled in time. Though there are many works in literature that investigate MG optimal capacity sizing, to our knowledge, our work is the first that utilizes the scheduling of programmable appliance to minimize MG investment costs. To establish the effectiveness of our method, we compare an optimal MG capacity sizing algorithm that utilizes appliances' programmability (*Opt-P*) with an algorithm that places appliances into operation as soon as they are ready without shifting in time or preempting their operation (NoSch-P). Our simulation results show that Opt-P reduces the investment cost by at least 42% compared to NoSch-P, when the ratio between the energy storage investment cost per kWh and the RES' investment cost per kW is greater or equal to 10.

I. INTRODUCTION

One of the main contributions of microgrids (MGs), which are small scale power systems comprising distributed energy sources and loads, is the MGs' improved reliability and resilience to catastrophic power outages. Combining MGs with renewable energy sources (RES), such as solar panels (SPs) and wind turbines (WTs), allows reduction of the energy costs and carbon emission ([1],[2]). However, the unpredictability of RES electricity generation is a great challenge to their integration into MGs. This is particularly relevant in the context of completely green village (CGV), which is an isolated residential MG, whose energy is produced exclusively by RES. A promising solution to stabilize RES' power generation is the adoption of energy storage system (ESS) and controllable loads ([3]), as well as electric vehicles (EVs) ([4]). EVs are a special type of controllable loads, which, similarly to the ESS, can absorb the extra energy generated by RES, and can later discharge this energy when needed ([5]). Schedulable loads allow matching the load profile to the RES's power generation curve.

A CGV is composed of smart homes, whose load demands comprise of spontaneous loads, such as lights, TVs, and microwave ovens, as well as in-advance programmable appliances, such as laundry machines, dishwashers, and EVs. The programmable appliances have power and timing demands, which, when violated, incur customer discomfort and dissatisfaction. In this work, we address the optimal planning problem of a CGV, where we seek to determine the minimum number of RES sources and the size of ESS needed to satisfy the smart homes' load demands in a cost-efficient manner, while meeting MG reliability requirement.

II. RELATED WORKS

Although deterministic MG planning and its operation have been studied extensively in the literature in the past (e.g., [6]–[8]), stochastic models are more suited to capture the uncertainty associated with renewable energy and with certain types of (programmable and nonprogrammable) loads. Hence, we utilize the Chance Constrained Programming (CCP) method to account for the randomness in the sizing problem constraints. To solve the sizing problem, we use the Monte Carlo Simulation (MCS) method to generate a large number of scenarios that represent the renewable energy and load demand realizations. However, unlike previous works where MCS is combined with scenario reduction processes to reduce the computational complexity ([9]–[11]), our MCS solution approach allows to increase the solution accuracy ([12]).

In [13], Bahramirad et al. utilizes the MCS method to determine the optimal size of ESS in a MG, while considering power shortage due to outage of thermal units and RES intermittency. Similarly, reference [14] seeks to determine the optimal size of ESS in order to schedule the commitment of fuel cell power plants, where a two-stage scenario-based stochastic model is used to deal with uncertainty from load demand and RES output power. However, both [13] and [14] only focus on ESS sizing, while our work considers the planning of RES (i.e., the number of RES elements) in addition to ESS sizing.

In [10], the authors presents a stochastic model for the capacity expansion of a remote MG in terms of wind farms, thermal generators and ESS; the MCS method coupled with scenario reduction is used to account for RES uncertainty. The reference [15] seeks to simultaneously minimize the total present net cost and carbon emission for a MG with diesel generators, SPs, WTs, and lead-acid batteries and CCP is used to ensure that the capacity shortage is below a certain confidence level. However, unlike our work, none of the above works exploits the appliance schedulability feature to further reduce the MG's investment costs.

The work in [16] combines the MCS method with Particle Swarm Optimization to determine the optimal capacity of distributed-generation system and battery for a smart home with time-shiftable loads. While [16] assumes a rule-based electricity managements system for the smart household, our work makes no such assumption. Rather, our work seeks to determine the scheduling of appliances that minimizes the CGV investment cost. Additionally, our work focuses on the optimal planning of a completely green MG, which is in contrast to works [13]–[16] that consider a MG with fossil-fueled generators or with connection to the main grid.

In summary, our work's contributions include:

1) Formulation of a CCP problem to determine the optimal number of RES elements (e.g., SPs and WTs) and the size of the ESS that minimize the investment costs of a CGV.
2) Design of a MCS-based algorithm to solve the formulated CCP problem.
3) Determination of the optimal scheduling for programmable appliances that minimizes the investment costs.
4) Investigation of the impact of appliance schedulability and ESS on investment costs.

III. NOMENCLATURE

Alphabetic Symbol	Definition
A	Solar panel total area (m^2)
a	Appliance (EV) earliest possible start time (arrival)
$B(.,.)$	The Beta function
C_{ESS}	ESS's maximum energy capacity (kWh)
ch	EV required charging time (hours)
C	ESS energy state (kWh)
d	Appliance/EV deadline
DoD_{max}	ESS maximum allowed depth of discharge
DoD_{min}	ESS minimum depth of charge
$f(.)$	Chance Constrained P objective function
$f_k(.)$	Solar panel probability density function
$f_w(.)$	Wind speed probability density function
$gi(.)$	Constraint function
H	Number of homes
I	Shape factor
IC_e	ESS rating cost ($/kWh)
IC	RES investment cost per kW ($/kW)
ir	Actual sun irradiation (kW/m^2)
IR_{max}	Maximum irradiation (kW/m^2)
J	Number of appliances per home
K	Number of solar panels
M	Total number of EVs
NP_{max}	Maximum number of Solar Panels observed
NP_{min}	Minimum number of Solar Panels observed
NS	Number of scenarios
NW_{max}	Maximum number of Wind turbines observed
NW_{min}	Minimum number of Wind turbines observed
Op	Optimal number of solar panels
OS	Optimal storage capacity (kWh)
Ow	Optimal number of Wind turbines
P_{ESS}	ESS maximum charging/discharging power (kW)
p	Appliance/EV/RES power consumption/transferred power /output power (kW)
PC	RES power capacity (kW)
PL	EV energy level (kWh)
PL^{max}	EV maximum allowed energy level (kWh)
p^{max}	Maximum energy transferrable to/from EV (kWh)
PL^{min}	EV minimum energy level (kWh)
P_{rate}	Wind turbine rated power (kW)
p_{ch}	ESS charging power (kW)
p_{dch}	ESS discharging power (kW)
r	Appliance operation duration (hours)
SC_{max}	Maximum storage capacity observed
SC_{min}	Minimum storage capacity observed
SF	Scale factor
SP	Schedulability parameter
T	24 hour scheduling period
u	Appliance operation status
v	Wind speed (m/s)
V_{in}	Wind turbine cut-in speed (m/s)
V_{out}	Wind turbine cut-out speed (m/s)
V_{rate}	Wind turbine rated wind speed (m/s)
vs	Binary variable that is 1 if EV is at home
W	Number of wind turbines
ws	Indicates EV charging status
x	n-dimensional decision variable

Greek Symbol	Definition
α and β	Shape parameters of the Beta distribution
γ	compares energy storage and RES' investment costs
λ	Confidence level
eff	ESS charging and discharging efficiency (%)
η	Solar panel's efficiency (%)

Subscript Symbol	Definition
k	Solar panel index
w	Wind turbine index
j	Appliance index
h/f	Home indices
m	EV index
t,i	time indices
ar	arrival
Tg	Target

IV. SYSTEM MODEL

We model a CGV that contains smart appliances, EVs, RES and ESS. We use a discrete time model, where each time slot represents an hour of operation and the optimization is performed over a period of $T = 24$ hours. We consider the load demand and RES generation characteristics over one year. The CGV investment cost comprises the purchasing costs and the installation costs of WTs and SPs, as well as the ESS' investment cost.

A. Monte Carlo Scenario Generation

MCS method can be used to account for uncertainty in the sizing problem. The main source of randomness in the sizing problem is the power production of RES and the load demand. Since the RES performance and load profile depend on weather conditions, we consider 4 representative days, each corresponding to one of the four season of the year ([10]).

The MCS method seeks to estimate the problem's random variables by evaluating a large number of representative scenarios. Each such a scenario is generated as an outcome of the random variables and represents a sample system state. Indeed, [12] indicates that the MCS approach is very suitable when analyzing large systems, such as power systems.

B. Chance-Constrained Programming

CCP is typically used to solve problems with constraint stochastic variables. Since constraints might be violated in some extreme conditions, CCP allows the solutions to violate the constraints to some degree, as long as the probability to meet these constraints is above an established confidence level. A typical CCP problem can be expressed as follows:

$$\begin{aligned} &\min f(x) \\ &s.t\ \Pr\{g_i(x,\zeta) \le 0,\quad i = 1,2,...\} \ge \lambda \end{aligned}, \tag{1}$$

where *f(x)* is an objective function, x is an n-dimensional decision variable, ζ is an m-dimensional random vector, $g_i : R^n \times R^m \to R$, and λ represents the required confidence level that takes values in the interval (0,1). The probability $\Pr\{g_i(x,\zeta) \le 0,\quad i = 1,2,...\} \ge \lambda$ represents the joint probability constraint over all the $g_i(x,\zeta) \le 0$ constraint functions.

C. RES Model

1) Wind Turbines

We model W identical wind turbines. Each wind turbine (WT) has a power generation capacity of PC_w [kW] and is associated with an investment cost per generated kW of power of IC_w[$/kW]. The wind turbine's output power at time t is mostly related to the wind speed, v [m/s]. To simulate the randomness of wind speed, Weibull probability density function (*pdf*) is used ([10]):

$$f_w(v) = \left(\frac{I}{SF}\right)\left(\frac{v}{SF}\right)^{I-1} \exp\left[-\left(\frac{v}{SF}\right)^{I}\right], \tag{2}$$

where *I, SF,* and v are shape factor, scale factor, and wind speed, respectively. Since the wind distribution parameters change with the seasons of the year, four different values are used for the shape factor and scale factor, as per empirical studies ([17]). The electric output of the wind turbine w, as a function of v, is expressed as:

$$p_w = \begin{cases} 0, & v < V_{in}\ or\ v \ge V_{out} \\ P_{rate}\dfrac{v - V_{in}}{V_{rate} - V_{in}}, & V_{in} \le v < V_{rate} \\ P_{rate}, & V_{rate} \le v < V_{out} \end{cases} \tag{3}$$

where V_{in} and V_{out} refer, respectively, to the turbine's cut-in speed (minimum wind speed) and cut-out speed (maximum wind speed) both in [m/s], established for safety reasons. P_{rate} and V_{rate} denote the turbine's rated power and its corresponding wind speed, respectively. When the wind speed is greater or equal to V_{out}, the turbine rotor is stopped, so as to prevent damage. Hence, as indicated by (3), the turbine's output power is zero once v is equal to or greater than V_{out}.

2) Solar Panels

We model K identical solar panels. Each solar panel (SP) unit has power generating capacity of PC_k [kW] and is also associated with an investment cost per generated kW of power of IC_k [$/kW], which includes purchasing and installation costs. The SP output power depends on the sun irradiation *ir* [kW/m^2], which is modelled by a Beta distribution function. The probability density function of the Beta distribution is ([18]):

$$f_k(ir) = \frac{1}{B(\alpha,\beta)}\left(\frac{ir}{IR_{\max}}\right)^{\alpha-1}\left(1 - \frac{ir}{IR_{\max}}\right)^{\beta-1}, \tag{4}$$

where $B(\alpha,\beta)$ is the Beta function, α and β are the shape parameters of the Beta distribution, and *ir* and IR_{max} are the actual sunlight and the maximum irradiation, respectively. The parameters α and β are calculated from the solar radiation mean (μ) and standard (σ) deviation values, as follows ([19]):

$$\beta = (1-\mu)\left[\frac{\mu(1+\mu)}{\sigma^2} - 1\right] \quad (5)$$
$$\alpha = \frac{\mu * \beta}{1-\mu}$$

Using *ir*, the solar panel's output power is found by:

$$p_k = \eta_k A_k ir, \quad (6)$$

where η_k and A_k represent the solar panel's efficiency (in %) and solar panel's total area [m^2], respectively.

D. Smart Home and Appliance Models

1) Non-Schedulable Load:

The smart homes' static load curve is due to non-programmable appliances, such as lights or TVs. We model the hourly static load using a load range, where the hourly load value is randomly chosen between a minimum and a maximum values using a uniform distribution function. Reference [20] provides an observed load range for hourly static load demand per house, as shown in Fig. 1.

2) Programmable Appliances:

We model H smart homes, where each smart home contain J programmable appliances, such as a dishwasher, a laundry machine, and a spin dryer. A programmable appliance's operation can be interrupted and rescheduled (i.e., shifted in time) in contrast to non-programmable appliances, whose operation cannot be altered once started. (As an example, of a programmable appliance operation, consider a washing machine that can be scheduled to operate anytime between 9:00am and 5:00pm, when the owner is at work, and needs 2 hours to finish its cycle.) Each appliance j in home h is characterized by the tuple $\{p_{h,j}, r_{h,j}, a_{h,j}, d_{h,j}\}$, where $p_{h,j}$ is the appliance j's power consumption in kW, $r_{h,j}$ is its operation duration (in hours), $a_{j,h}$ is its earliest possible start time, and $d_{h,j}$ is the appliance's latest possible finish time; i.e., $d_{h,j}$ provides a deadline by which appliance j in home h has to complete its operation.

The start time $a_{h,j}$ and the deadline $d_{h,j}$ are modelled as random variables and are generated as follows: $a_{h,j}$ is a random integer drawn from the discrete uniform distribution in the interval $[1, T\text{-}r_{h,j}+1]$, and $d_{h,j}$ is a discrete uniform random integer in interval $[a_{h,j}+r_{h,j}-1, \min(a_{h,j}+SP*r_{h,j}, T)]$. SP is an integer parameter and represents the schedulability of the programmable appliances; that is the flexibility in appliance scheduling increases as SP increases.

We use the variable $u_{h,j,t}$ to show the operation status of appliance j; $u_{h,j,t}$ is 1 if appliance j in home h is operating during slot t and 0 otherwise. In order for a programmable appliance to complete its operation, the following must hold:

$$\sum_{t=a_{h,j}}^{d_{h,j}} u_{h,j,t} = r_{h,j} \quad (7)$$

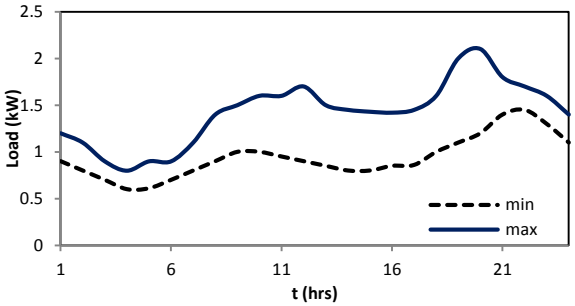

Fig. 1: Static Load Range per House per Day [20]

3) Electric Vehicle

EVs are a special type of programmable appliances that based on their operation, can charge/discharge electricity. Each of the M EVs belongs to a home h and is characterized by the tuple $\{PL_{m,ar}, PL_{m,Tg}, a_m, d_m, p_m^{\max}, f_m\}$. The a_m and d_m values indicate EV's arrival time at the MG and its scheduled departure time, respectively. f_m identifies the smart home that the m^{th} EV belongs to, where $f_m \in [1,\ldots,H]$. $PL_{m,ar}$ refers to the m^{th} EV arrival energy level, while $PL_{m,Tg}$ denotes the m^{th} EV's departure target energy level. We denote as $p_m^{\max}$ the maximum amount of energy transferrable to/from the m^{th} EV during time slot t. Here, we note that $PL_{m,ar}, PL_{m,Tg}, a_m$, and d_m are all random variables in the planning problem generated as follows: $PL_{m,ar}$ is a uniform random number in the interval $[PL_m^{\min}, PL_m^{\max}]$, where $PL_m^{\min}$ and $PL_m^{\max}$ are the minimum battery discharge level and the maximum battery charge level, respectively. $PL_{m,Tg}$ is a random number drawn from a uniform distribution in the interval $[PL_{m,ar}, PL_m^{\max}]$. The m^{th} EV's arrival time a_m is a random integer in the interval $[1, T\text{-}ch_m]$ following a discrete uniform distribution, where ch_m is the required charging time needed to achieve the target power level; ch_m is obtained by $(PL_{m,Tg} - PL_{m,ar})/p_m^{\max}$. d_m is a random integer selected from a discrete uniform distribution in the interval $[a_m + ch_m - 1, \min(a_m + SP * ch_m, T)]$.

The m^{th} EV's energy level in slot t, $PL_{m,t}$, is calculated as:

$$PL_{m,t} = PL_{m,ar} - \sum_{i=1}^{t} p_{m,i} * vs_{m,i} * ws_{m,i}, \quad (8)$$

where $vs_{m,i}$ is a binary variable that is 1 if the EV is at home (in the interval $[a_m, d_m]$), and zero otherwise. $ws_{m,i}$ is 1 if the m^{th} EV is charging, -1 if the EV is discharging, and zero if the EV is idle. $p_{m,i}$ is the energy transferred to/from the EV during the i^{th} hour. For safety and longevity, each EV should not charge beyond it capacity $PL_m^{\max}$, discharge below its minimum discharge level $PL_m^{\min}$, or transfer more than $p_m^{\max}$ kWh during an hour:

$$PL_m^{\min} \le PL_{m,t} \le PL_m^{\max}$$
$$0 \le p_{m,t} \le p_m^{\max} \quad (9)$$

The scheduling of EV's charging has to ensure that each EV has the target energy level before it departs again for driving:

$$PL_{m,d_m} \ge PL_{m,Tg} \quad (10)$$

E. Energy Storage System

The ESS investment cost per kWh of stored energy is the energy rating cost, IC_e [$/kWh] ([21]). We use the parameter γ to compare the ESS investment cost and the renewable energy investment cost; i.e., $\gamma = IC_e / \langle IC_w, IC_k \rangle$, where $\langle IC_w, IC_k \rangle$ is a simple arithmetic average of IC_w and IC_k. We want to analyze how the investment costs, the RES capacity and the ESS capacity, change as γ varies. ESS's charging power $p_{t,ch}$ and discharging power $p_{t,dch}$ in slot t are subject to the following minimum and maximum constraints:

$$0 \le p_{t,ch}, p_{t,dch} \le P_{ESS}, \quad (11)$$

where P_{ESS} is the maximum ESS charging/discharging power. ESS' state (the amount of energy stored) C_t in slot t is found by (12) and, to ensure repeatability from a day to the next, is assumed to be the same at the beginning and at the end of a day, as indicated by (13). C_t is also restricted by ESS capacity limits as shown by (14). The parameter *eff* is the charging and discharging efficiency of the ESS (in %), while DoD_{min} and DoD_{max} are the minimum and the maximum allowed depth of discharge, respectively; C_{ESS} is ESS's maximum energy capacity. The ESS' state of charge is maintained within an allowed range, as specified by the depth of discharge values.

$$C_t = C_{t-1} + eff \cdot p_{t,ch} - \frac{1}{eff} p_{t,dch} \quad (12)$$

$$C_1 = C_T \quad (13)$$

$$(1 - DoD_{\max}) C_{ESS} \le C_t \le (1 - DoD_{\min}) C_{ESS} \quad (14)$$

F. Power Balance

The generated wind and solar powers are random variables that depend on the wind speed and the irradiation stochastic variables, respectively. In addition, the load demand is also stochastic, and depends on the appliances' earliest start times and deadlines as well EVs' arrival and departure times. Hence, the power balance constraints are expressed by probabilistic equations. This allows the following constraints to be met with a certain confidence level:

$$\Pr\{g_t(x^t, \zeta^t) \le 0, \forall t\} \ge \lambda$$
$$g_t(x^t, \zeta^t) := \sum_{h=1}^{H} \sum_{j=1}^{J_h} u_{h,j,t} p_{h,j} - \sum_{m=1}^{M} p_{m,t} vs_{m,t} ws_{m,t} + p_t^{ch} - p_t^{dch} - W * p_{w,t} - K * p_{k,t} \quad (15)$$

$$u_{h,j,t}, vs_{m,t} \in \{0,1\}, \quad \forall t, \forall h, \forall j, \forall s1$$
$$p_{m,t} \ge 0, ws_{m,t} \in \{-1,0,1\} \quad \forall t, \forall m, \forall j \quad (16)$$

where, as defined above, λ is the constraint's confidence level. Vector x^t is made up of variables $\{W,K,C_{ESS}\}$, as well as variables $u_{h,j,t}$ and $ws_{m,t}$. The random vector ζ^t results from the randomness in variables $vs_{m,t}$ (uncertainty due to EVs arrival and departure times), $p_{w,t}$ (intermittency due to wind speed), and $p_{k,t}$ (intermittency due to solar irradiation). Constraint (15) states that the probability of the power generated by the renewable sources and the available ESS energy meeting the load demand in every timeslot t has to be greater or equal to the predefined value of λ. We restrict the variable to their respective ranges by (16).

G. Problem Statement

Our goal is to minimize the MG investment cost, while ensuring that smart homes load is guaranteed to be satisfied with probability λ.

$$\min (W * PC_w IC_w + K * CP_k PC_k + IC_e C_{ESS}^s) \quad (17)$$
s.t. (1)–(16) hold.

V. SOLUTION METHODOLOGY

The formulated problem has a linear objective function, and linear constraints, with some variables restricted to be integers. Hence, we could solve the problem in (17) as mixed integer linear programming problems (MILP). The difficulty lies with the joint probability constraint (15). Equation (15)'s closed form is intractable, since the joint spatio-temporal probability distribution of the wind and the solar powers is not known and is generally non-convex ([22]).

To solve (17), we use the MCS to generate scenarios that capture the uncertainties in the wind speed, the solar irradiation, and the load demand. Below is the description of the MCS-based designed algorithm:

1) Generate *NS* scenarios, where each scenario *s* is characterized by a wind speed sample w_s, a solar irradiation sample ir_s, and a load profile sample l_s. Assuming that all the scenarios are independent, we set the probability of each scenario to be *1/NS*.

2) Solve the sizing problem for all the *NS* scenarios; for each scenario *s*, we save the values for the computed optimal number of WTs and SPs (Ow_s and Op_s, respectively), the optimal ESS capacity OS_s, and the optimal cost OC_s. We also keep track of NW_{min} and NW_{max}, the minimum number and the maximum number of wind turbines observed among returned solutions; similarly, we also record NP_{min} and NP_{max} – the minimum and the maximum number of solar panels observed, and SC_{min} and SC_{max} – the minimum and the maximum ESS capacity, as returned by the solutions of the scenarios (SC_{min} is rounded down to the closest integer, and SC_{max} is rounded up to the closest integer).

3) Given the confidence level λ, we determine the minimal cost solution that ensures that λ*100% of the scenarios are satisfied as follows:

For $i = NW_{min}$ up to NW_{max}
  For $j = NP_{min}$ up to NP_{max}
    Prob = 0; k = SC_{min};
    Opt-Cost = 0; Opt-NW = 0; Opt-NP = 0; Opt-SC = 0;
    While ($k <= SC_{max}$)
      s = 1;
      While (s <= NS)
        If ($Ow_s <= i$ and $Op_s <= j$ and $OS_s <= k$)
          Prob = Prob + Pr(s);
        End
        s = s+1;
      End
      If (Prob >= λ)
        Find the sizing cost using (17) given:
        i WTs, j SPs and size k for storage capacity.
        If (Opt-Cost > temp-Cost or Opt-Cost = 0);
          Opt-NW = i; Opt-NP = j; Opt-SC = k;
          Opt-Cost = temp-Cost;
        End
      End
      $k = k$+1;
    End
  End
End

The "**While** (k <= SC_{max})" seeks to determine the portion of the scenarios whose load can be satisfied by a MG composed by x WTs, y SPs, and a ESS of size z; that is, scenarios than require x or less WTs, y or fewer SPs, and an ESS of size z or smaller.

VI. SIMULATION PARAMETERS

A. RES Parameters:

The RES parameters are shown in Table I; we consider all WTs to be identical and all SPs to be identical. As we mentioned in Section IV, we model the wind speed distribution by considering four different values for the scale factor and shape factor, as shown in Table II. For the solar panel simulations, we use the 2010 solar irradiation mean and standard deviation values of the Boise Air Terminal site in Idaho obtained from the National Solar Radiation Data Base ([23]).

B. EV and ESS Parameters

EVs and ESS's parameters are as shown in Table III. We assume that each home has two EVs. Since we considered a total of 5 smart homes, we modeled 10 EVs in total. In these simulations, the schedulability parameter SP is set to 5.

C. Static Load

Since, as shown in Fig. 1, the gap between the hourly minimum and the maximum static load is negligible (no greater than 1 kW), we assume for simplicity that each home's static load curve is equal to the average of the max and the min values.

D. Appliance Parameters

Table IV describes the appliance parameters. All the appliances can start operating anytime during the day based on the residents' choice. With SP = 5, the deadline for each appliance is chosen as $min(T, a_j+5*r_j)$, where a_j and r_j are the start time and the duration of the appliance j operation, respectively. The residents' appliance use varies with the seasons of the year; in particular, we assume that the space heater is only operated during the winter, while the air conditioner is used during the other three seasons. Additionally, we assume that the air conditioner usage doubles during the summer. Table V shows the total number of operations per appliance type per season of the 5 smart homes. As an example, Fig. 2 illustrates one sample of the load profile for non-static load, resulting from the appliance power demand during the summer season. When compared to static load in Fig.1, we note that the appliance load demand is significantly more irregular compared to the static load demand.

Table I: RES Operation Parameters

Wind Turbine	Solar Panel
Cut-in speed (m/s) = 3.5	Area (m^2) = 100
Cut-out speed (m/s) = 25	Efficiency (%) = 20
Rated speed (m/s) = 14	Max Power Capacity (kW) = 20
Rated Power (kW) = 20	Investment Cost ($/kW) = 200
Investment Cost ($/kW) = 200	

Table II. Wind Speed Distribution Factors [10]

Season	Winter	Spring	Summer	Fall
I	1.4	1.2	1.1	1.3
SF	9	8	7.5	8.5

Table III: EVs and ESS Parameters

EV Parameters (kWh)	ESS Parameters
Min Capacity = 3	Charging/discharging efficiency = 0.9
Max Capacity = 15	DoD_{max} = 1; DoD_{Min} = 0
Charging Rate = 3	Energy rating Cost ($/kWh) = 200

Table IV: Appliance Parameters [24]

Appliance Type	p_j (kW)	r_j (hours)
Dish-Washer	2.8	2
Spin Dryer	2.5	3
Air Conditioner	1	4
Laundry Machine	2.5	3
Water Heater	5	2
Space Heater	3.4	3

Table V: Total Number of Daily Operations per Appliance Type per Season

Season	Winter	Spring	Summer	Fall
Dish-Washer	5	5	5	5
Spin Dryer	5	5	5	10
Air Conditioner	-	10	20	10
Laundry Machine	5	5	5	5
Water Heater	10	10	10	10
Space Heater	20	-	-	-

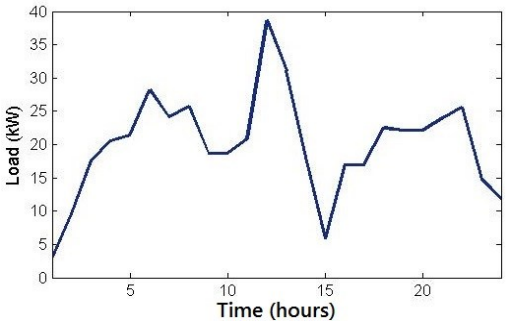

Fig. 2: Non-Static Load for Winter Season

E. Scenario Generation

The scenarios were generated following the MCS method. For each season, we generate 25,000 scenarios, where each scenario is characterized by a wind speed sample, a solar irradiance sample, and a load demand sample. We simulate a total of 100,000 scenarios; that is *NS* = 100,000. As aforementioned, previous works that uses MCS method usually starts with a large number of scenarios, and then uses some scenario reduction process to decrease the number of scenarios (usually to less than 10 scenarios). This in turn reduces the solution accuracy. Thus, by using a large number of samples in our solution method, we improve the solution accuracy.

F. Comparison Schemes

We compared two planning schemes. The first scheme is the optimal planning scheme (Opt-P) that utilizes appliances' programmability, as well as EVs and ESS' charging/discharging capacity, so as to minimize the total investment cost. We compare the Opt-P scheme to a planning scheme that does not perform any load scheduling (NoSch-P); NoSch-P places appliances and EVs into operation as soon as they are ready, without shifting in time or interrupting their operation.

VII. SIMULATION RESULTS

A. Varying Confidence Level

Fig. 3 shows the cost reduction of the Opt-P scheme over the NoSch-P scheme, as the confidence level λ varies. For instance, λ = 0.9 mean that the returned solution has to satisfy the load demand for at least 90% of the scenarios. In these simulations $\gamma = 1$, which means that the ESS investment cost per kWh is equal to RES' investment cost per kW. Fig. 3 shows that as long as λ is less or equal to 0.9, Opt-P reduces the investment costs by 20% or more in comparison to NoSch-P scheme.

As shown in Fig. 4 and Fig. 5, when $\lambda \leq 0.9$ NoSch-P generally requires more resources than Opt-P; in particular, NoSch-P's always needs more ESS capacity (24 kWh or more) in comparison to Opt-P, which explains the Opt-P's cost reduction of 20% or more in Fig. 3. Thus, as long as we allow the power balance constraint (15) to be violated in 10% or more of scenarios, we save at least 20% in cost reduction with appliance scheduling. When λ > 0.9, the difference in RES and ESS capacity needed by Opt-P and NoSch-P diminishes (Fig. 5 and Fig. 6), which explains the decrease in Opt-P's performance in Fig. 3.

B. Varying γ

In this section, we compare the Opt-P and the NoSch-P schemes, while varying γ and maintaining a confidence level of 90% ($\lambda = 0.9$). As demonstrated in Fig. 6, Opt-P outperforms NoSch-P by 42% or more when $\gamma \geq 10$ (ESS investment cost per kWh is 10 times greater or more in comparison to the investment cost per kW of the RES). For $\gamma = 1$, Opt-P needs a total number of 7 RES and 113 kWh of storage, while NoSch-P needs 9 RES and 137 kWh of storage (Fig. 7 and Fig. 8). Through the use of load scheduling, Opt-P is able to reduce the required number of RES and the storage capacity, thus decreasing the investment cost by 20%.

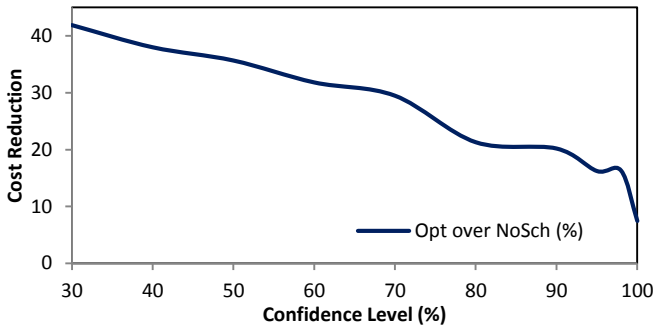

Fig. 3: Cost Reduction Comparison

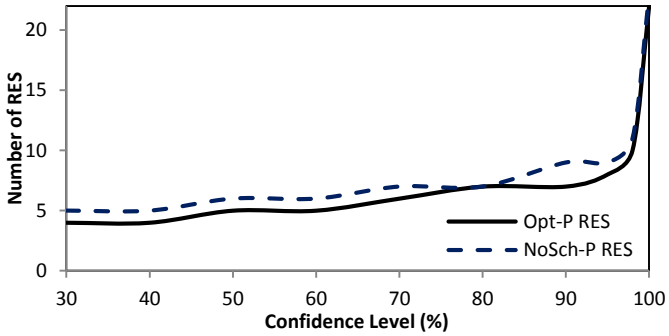

Fig. 4: Comparison of Number of RES

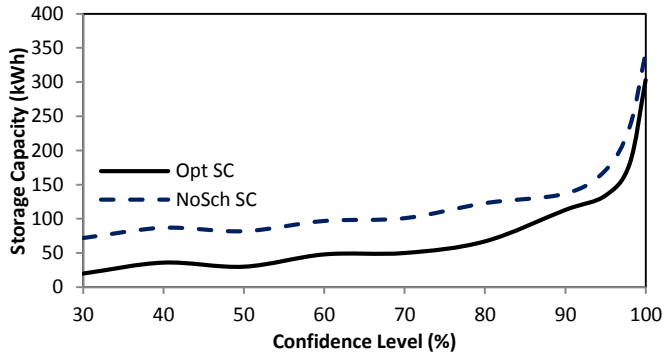

Fig. 5: Storage Capacity Comparison

Fig.7 shows that Opt-P's ESS investment cost is always less than NoSch-P's and decreases as ESS becomes more costly than RES. For $\gamma \geq 10$, Opt-P uses load scheduling to decrease its ESS' capacity to 55 kWh or less. However, NoSch-P always needs at least 90 kWh or more for energy storage when $\gamma \geq 10$, since it does not utilize load scheduling. In addition, Fig. 8 illustrates that for $\gamma \geq 10$, NoSch-P generally needs more RES compared to Opt-P. This explains Opt-P's significant cost reduction over NoSch-P in Fig. 6 (more than 42%) when $\gamma \geq 10$. Fig. 8 also shows that as the cost of energy storage increases, the investment in RES increases for both Opt-P and NoSch-P to take advantage of the relatively cheaper energy generation costs (compared to energy storage).

When $10\text{^}{-5} < \gamma \leq 0.01$, NoSch-P is able to utilize the cheap storage, so as to reduce the number of RES needed, thus only incurring negligible cost penalties in comparison to Opt-P (7% or less as illustrated in Fig. 6). For $\gamma = 10\text{^}{-5}$ and $\gamma = 10\text{^}3$, NoSch-P had to satisfy 95% of scenarios to satisfy $\lambda = 0.9$, while Opt-P only met 90% of all cases (for the other γ points in Fig. 6, NoSch-P and Opt-P's returned confidence levels that were in range 90%-92%). This confidence level of 95% explains the sharp increase in NoSch-P's number of RES when $\gamma = 10\text{^}{-5}$ and $\gamma = 10\text{^}3$ compared to other nearby NoSch-P points. For instance, from $\gamma = 10\text{^}3$ to $\gamma = 10\text{^}5$, NoSch-P's number of RES does not change, while from $\gamma = 10\text{^}1$ to $\gamma = 10\text{^}3$, NoSch-P's number of RES increases by 690 RES (Fig. 8). This explains the non-monotonic character of Opt-P performance over NoSch-P at these points in Fig. 6, since NoSch-P investment cost greatly increases.

On the other hand, for $\lambda = 0.7$, Opt-P and NoSch-P returned confidence level values that were in the interval 70% – 72%. This explains why, as illustrated in Fig 9, Opt-P's performance over NoSch-P increase monotonically when compared to the curve for $\lambda = 0.9$. Hence, we observe that if both schemes are evaluated at exactly the same confidence level or within 0.02 of the required confidence level, then Opt-P's performance over NoSch-P increases monotonically with the increase in γ values. Hence, the curve for $\lambda = 0.9$ in Fig. 6 and 9 would be monotonically increasing if we simulated a larger number of scenarios that would allow to evaluate both Opt-P and NoSch-P at exactly $\lambda = 0.9$ or within 0.02 of this value.

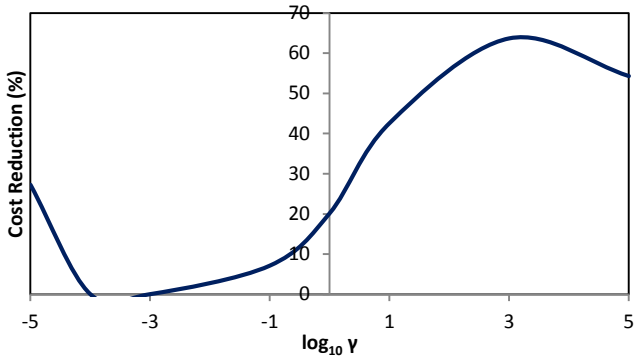

Fig. 6: Opt-P Cost Reduction Comparison as γ Varies

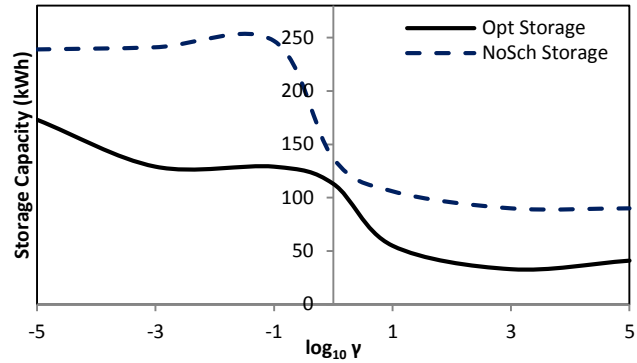

Fig. 7: Energy Storage Comparison

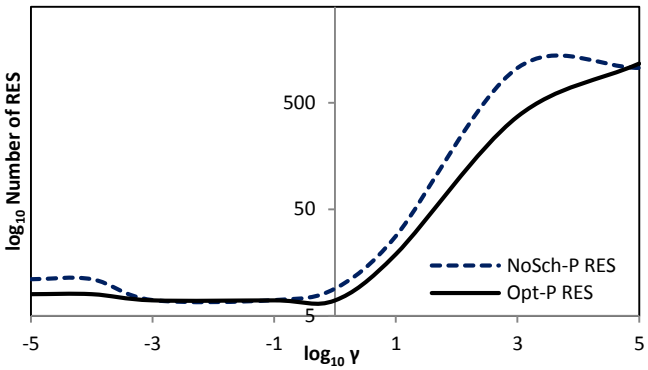

Fig. 8: Comparison of Number of RES

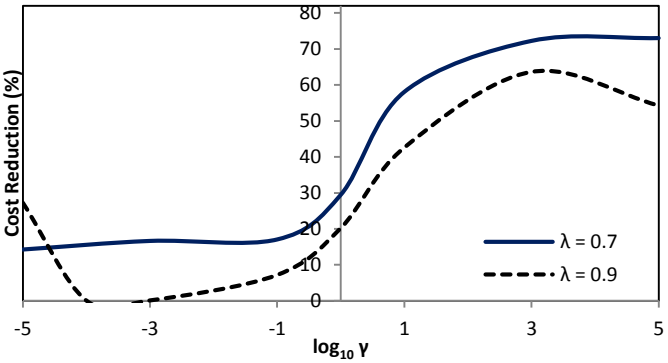

Fig. 9: Opt-P Cost Reduction for $\lambda = 0.7$ versus $\lambda = 0.9$

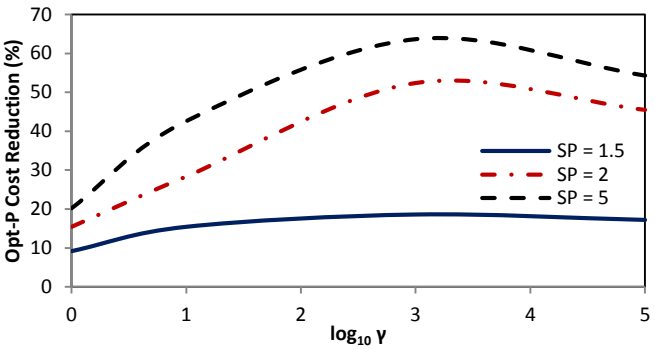

Fig. 10: Opt-P Performance as *SP* Varies

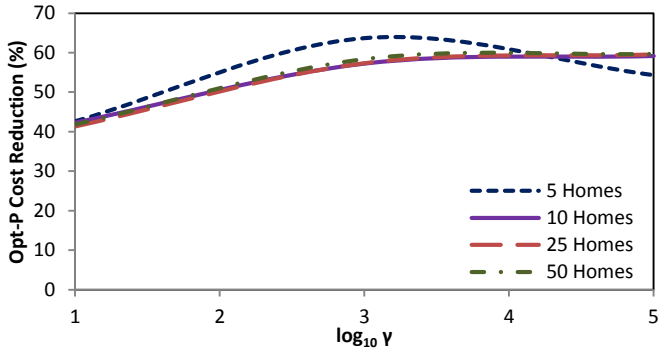

Fig. 11: Opt-P Performance as the Load Increases

C. Varying *SP*

In this section, we compare Opt-P to NoSch-P while varying the schedulability parameter *SP* and while maintaining the confidence level at 90% ($\lambda = 0.9$). Fig. 10 shows that Opt-P's cost reduction for *SP*=1.5 is significantly lower compared to when *SP* = 5 (*SP* = 1.5 mean that the deadline for each programmable appliance *j* is within 1.5* $r_{h,j}$, where $r_{h,j}$ is the appliance's duration of operation). In fact, Opt-P's cost reduction was always less or equal to 18% relative to the NoSch-P scheme for *SP* = 1.5. However, for *SP* = 2 Opt-P registers a cost reduction of 28% or more when $\gamma \geq 10$. Hence, we observe that Opt-P leads to higher cost reduction when the residents allows for more flexibility in their appliance scheduling. In particular, when energy storage is more expensive that renewable energy, we observe considerable cost savings whenever appliances' deadlines are at least within double of their operation duration ($d_{h,j} = min(a_{h,j}+2*r_{h,j}, T)$).

D. Varying Load

Fig. 11 illustrates Opt-P's cost reduction over NoSch-P as the load demand increases with the number of homes. For these simulations, $\gamma \geq 10$ (the energy storage investment cost per kWh is 10 times greater than RES' investment cost per kW). The confidence level was set to 90% (λ = 0.9). We observe that Opt-P cost reduction remains greater than 41% even as the load demand increases (from a 5 home MG to a 50 home MG) and γ varies. Hence, we note that even in medium size MGs, Opt-P's is able to schedule all the CGV's programmable appliances to decrease the investment cost.

VIII. CONCLUSION

In summary, our work demonstrates that the investment cost of a completely green MG with smart homes can be significantly reduced by accounting for the programmability of smart appliances. In particular, when the ESS investment cost per kWh is 10 time greater or more in comparison to the RES' investment per kW, we observed a cost reduction of 41% or more for small to medium size MGs (MGs that have 5 to 50 homes). When the ESS is cheaper than the RES' investment cost, NoSch-P utilizes the low-cost ESS to decrease the number of RES needed, thus only incurring 7% or less in cost increases. Our results also demonstrated that the greatest cost savings were observed when the confidence level was less or equal to 0.9; that is when we allowed the load demand to be violated in 10% or more of the systems realization scenarios. Varying the appliances' schedulability parameter *SP*, we also noted that cost savings decreased as the appliances' scheduling flexibility decreased, but as long as *SP* ≥ 2, there is a significant cost reduction due to the appliances' programmability.

REFERENCES

[1] "MICROGRIDS - Large Scale Integration of Micro-Generation to Low Voltage Grids," *EU Contract ENK5-CT-2002-00610, Technical Annex*. [Online]. Available: http://microgrids.eu/micro2000/presentations/19.pdf. [Accessed: 24-Sep-2014].

[2] M. Shahidehpour and J. F. Clair, "A Functional Microgrid for Enhancing Reliability, Sustainability, and Energy Efficiency," *Electr. J.*, vol. 25, no. 8, pp. 21–28, Oct. 2012.

[3] B. Battke, T. S. Schmidt, D. Grosspietsch, and V. H. Hoffmann, "A review and probabilistic model of lifecycle costs of stationary batteries in multiple applications," *Renew. Sustain. Energy Rev.*, vol. 25, pp. 240–250, Sep. 2013.

[4] D. B. Richardson, "Electric vehicles and the electric grid: A review of modeling approaches, Impacts, and renewable energy integration," *Renew. Sustain. Energy Rev.*, vol. 19, pp. 247–254, Mar. 2013.

[5] F. Mwasilu, J. J. Justo, E.-K. Kim, T. D. Do, and J.-W. Jung, "Electric vehicles and smart grid interaction: A review on vehicle to grid and renewable energy sources integration," *Renew. Sustain. Energy Rev.*, vol. 34, pp. 501–516, Jun. 2014.

[6] B. S. Borowy and Z. M. Salameh, "Methodology for optimally sizing the combination of a battery bank and PV array in a wind/PV hybrid system," *IEEE Trans. Energy Convers.*, vol. 11, no. 2, pp. 367–375, Jun. 1996.

[7] O. Hafez and K. Bhattacharya, "Optimal planning and design of a renewable energy based supply system for microgrids," *Renew. Energy*, vol. 45, pp. 7–15, Sep. 2012.

[8] E. Ghiani, C. Vertuccio, and F. Pilo, "Optimal sizing and management of a smart Microgrid for prevailing self-consumption," in *2015 IEEE Eindhoven PowerTech*, 2015, pp. 1–6.

[9] A. Botterud, Z. Zhou, and J. Wang, "Use of wind power forecasting in operational decisions," *Argonne Natl. …*, 2011.

[10] E. Hajipour, M. Bozorg, and M. Fotuhi-Firuzabad, "Stochastic Capacity Expansion Planning of Remote Microgrids With Wind Farms and Energy Storage," *IEEE Trans. Sustain. Energy*, vol. 6, no. 2, pp. 491–498, Apr. 2015.

[11] W. L. de Oliveira, C. Sagastizábal, D. D. J. Penna, M. E. P. Maceira, and J. M. Damázio, "Optimal scenario tree reduction for stochastic streamflows in power generation planning problems," *Optim. Methods Softw.*, vol. 25, no. 6, pp. 917–936, Dec. 2010.

[12] L. Wu, M. Shahidehpour, and T. Li, "Stochastic Security-Constrained Unit Commitment," *IEEE Trans. Power Syst.*, vol. 22, no. 2, pp. 800–811, May 2007.

[13] S. Bahramirad, W. Reder, and A. Khodaei, "Reliability-Constrained Optimal Sizing of Energy Storage System in a Microgrid," *IEEE Trans. Smart Grid*, vol. 3, no. 4, pp. 2056–2062, Dec. 2012.

[14] S. Mohammadi and A. Mohammadi, "Stochastic scenario-based model and investigating size of battery energy storage and thermal energy storage for micro-grid," *Int. J. Electr. Power Energy Syst.*, vol. 61, pp. 531–546, Oct. 2014.

[15] B. Hong, L. Guo, B. Jiao, W. Liu, and C. Wang, "Multi-objective stochastic optimal planning method for stand-alone microgrid system," *IET Gener. Transm. Distrib.*, vol. 8, no. 7, pp. 1263–1273, Jul. 2014.

[16] S. Kahrobaee, S. Asgarpoor, and W. Qiao, "Optimum Sizing of Distributed Generation and Storage Capacity in Smart Households," *IEEE Trans. Smart Grid*, vol. 4, no. 4, pp. 1791–1801, Dec. 2013.

[17] I. Y. . Lun and J. C. Lam, "A study of Weibull parameters using long-term wind observations," *Renew. Energy*, vol. 20, no. 2, pp. 145–153, Jun. 2000.

[18] X. Lin, P. Li, J. Ma, Y. Tian, and D. Su, "Dynamic optimal dispatch of combined heating and power microgrid based on leapfrog firefly algorithm," in *2015 IEEE 12th International Conference on Networking, Sensing and Control*, 2015, pp. 416–420.

[19] M. Mazidi, A. Zakariazadeh, S. Jadid, and P. Siano, "Integrated scheduling of renewable generation and demand response programs in a microgrid," *Energy Convers. Manag.*, vol. 86, pp. 1118–1127, Oct. 2014.

[20] Pacific Gas and Electrical (PG&E), "Residential load profiles," 2002. [Online]. Available: http://www.pge.com/nots/rates/2002_static.shtml#topic1.

[21] S. X. Chen, H. B. Gooi, and M. Q. Wang, "Sizing of Energy Storage for Microgrids," *IEEE Trans. Smart Grid*, vol. 3, no. 1, pp. 142–151, Mar. 2012.

[22] G. Martinez, Y. Zhang, and G. B. Giannakis, "An efficient primal-dual approach to chance-constrained economic dispatch," in *2014 North American Power Symposium (NAPS)*, 2014, pp. 1–6.

[23] NREL, "National Solar Radiation Data Base." [Online]. Available: http://rredc.nrel.gov/solar/old_data/nsrdb/.

[24] S. Rajakaruna, F. Shahnia, and A. Ghosh, Eds., *Plug In Electric Vehicles in Smart Grids*. Singapore: Springer Singapore, 2015.

